Available online on 15.11.2022 at <http://jddtonline.info>

Journal of Drug Delivery and Therapeutics

Open Access to Pharmaceutical and Medical Research

Copyright © 2022 The Author(s): This is an open-access article distributed under the terms of the CC BY-NC 4.0 which permits unrestricted use, distribution, and reproduction in any medium for non-commercial use provided the original author and source are credited



Open Access Full Text Article



Research Article

ADMETox-informatics of Plant Derived Octadecanoic Acid (Stearic Acid) from Ethyl Acetate Fraction of *Moringa oleifera* Leaf Extract as a Natural Lead for Next Generation Drug Design, Development and Therapeutics

Murugan M.¹, Kalaimathi RV.¹, Krishnaveni K.², Basha AN.¹, Gilles A Pallan.¹, Kandeepan C.¹, Senthilkumar N.³, Mathialagan B.⁴, Ramya S.⁴, Jayakumararaj R.^{5*}, Loganathan T.⁶, Pandiarajan G.⁷, Kaliraj P.⁸, Sutha S.⁹, Kandavel D.¹⁰, Grace Lydial Pushpalatha G.¹¹, Abraham GC.¹² Ram Chand Dhakar¹³

¹ PG & Research Department of Zoology, Arulmigu Palaniandavar College of Arts & Culture, Palani – 624601, TN, India

² Department of Zoology, GTN Arts & Science College, Dindigul - 624005, TN, India

³ Institute of Forest Genetics & Tree Breeding (IFGTB), ICFRE, Coimbatore – 641002, TN, India

⁴ PG Department of Zoology, Yadava College (Men), Thiruppalai - 625014, Madurai, TN, India

⁵ Department of Botany, Government Arts College, Melur – 625106, Madurai District, TN, India

⁶ Department of Plant Biology & Plant Biotechnology, LN Government College (A), Ponneri, TN, India

⁷ Department of Botany, Sri S Ramasamy Naidu Memorial College (A), Sattur - 626203 TN, India

⁸ Department of Zoology, Sri S Ramasamy Naidu Memorial College (A), Sattur - 626203 TN, India

⁹ Department of Medicinal Botany, Govt. Siddha Medical College, Palayamkottai, Tamil Nadu, India

¹⁰ Government Arts College for Men (Autonomous), Nandanam, Chennai – 600 035, Tamil Nadu, India

¹¹ PG Department of Botany, Sri Meenakshi Government Arts College, Madurai – 625002, TN, India

¹² PG & Research Department of Botany, The American College, Madurai – 625002, Tamil Nadu, India

¹³ Hospital Pharmacy, SRG Hospital & Medical College Jhalawar-326001, Rajasthan, India

Article Info:



Article History:

Received 26 Sep 2022
Reviewed 30 Oct 2022
Accepted 09 Nov 2022
Published 15 Nov 2022

Cite this article as:

Murugan M, Kalaimathi RV, Krishnaveni K, Basha AN, Gilles A Pallan, Kandeepan C, Senthilkumar N, Mathialagan B, Ramya S, Jayakumararaj R, Loganathan T, Pandiarajan G, Kaliraj P, Sutha S, Kandavel D, Grace Lydial Pushpalatha G, Abraham GC, Dhakar RC, ADMETox-informatics of Plant Derived Octadecanoic Acid (Stearic Acid) from Ethyl Acetate Fraction of *Moringa oleifera* Leaf Extract as a Natural Lead for Next Generation Drug Design, Development and Therapeutics, Journal of Drug Delivery and Therapeutics. 2022; 12(6):129-141

DOI: <http://dx.doi.org/10.22270/jddt.v12i6.5677>

*Address for Correspondence:

Dr R Jayakumararaj, Department of Botany, Government Arts College, Melur – 625106, Madurai District, TN, India

Abstract

In-silico Computer-Aided Drug Design (CADD) significantly relies on cybernetic screening of Plant Based Natural Products (PBNPs) as a prime source of bioactive compounds/ drug leads due to their unique chemical structural scaffolds and distinct functional characteristic features amenable to drug design and development. In the Post-COVID-Era a large number of publications have focused on PBNPs. Moreover, PBNPs still remain as an ideal source of novel therapeutic agents of GRAS standard. However, a well-structured, in-depth ADME/Tox profile with deeper dimensions of PBNPs has been lacking for many of natural pharma lead molecules that hamper successful exploitation of PBNPs. In the present study, ADMET-informatics of Octadecanoic Acid (Stearic Acid - SA) from ethyl acetate fraction of *Moringa oleifera* leaves has been envisaged to predict ADMET and pharmacokinetics (DMPK) outcomes. This work contributes to the deeper understanding of SA as major source of drug lead from *Moringa oleifera* with immense therapeutic potential. The data generated herein could be useful for the development of SA as plant based natural product lead (PBNPL) for drug development programs.

Keywords: *Moringa oleifera*; Bioactive Substances; Octadecanoic Acid; Stearic Acid; ADME/Tox; Natural Product Based Drug Lead; PBNPs

INTRODUCTION

Chemically, Octadecanoic Acid/ Stearophanic Acid (Stearic Acid) is one of the most common long-chain fatty acids, found in combined form in animal and vegetable fats. Commercial "Stearic Acid" contains equal amounts of Stearic Acid (SA) and Palmitic Acid (PA) and small amounts of Oleic Acid (OA)¹. It is one of the common saturated fatty acid naturally obtained from plant sources with the molecular formula C₁₈H₃₆O₂^{2,3}. Stearic Acid is widely used as the major component in the production of washing detergents, soaps, and personal care products (PCP) such as cosmetics, shampoos and shaving creams. However, it must be noted that the detergent soaps are not directly made from SA, but through saponification of triglycerides of Stearic Acid Esters (SAE)^{2,3}. SAE with ethylene glycol, glycol stearate, and glycol di-stearate are used in the preparation of shampoos, soaps, and other cosmetic products to impart a pearly effect. They are added to the product in the molten form and allowed to crystallize under specific conditions so as to impart desirable effect in the products. Best available detergents in the market are obtained from amides/ quaternary alkyl-ammonium derivatives of SAE^{2,3}.

High fatty acid content in *Moringa oleifera* seed oil (MOSO) has rarely been exploited by Fast-Moving Consumer Goods (FMCG) industries for the production of Food Grade Consumable Products (FGCP) due to low melting point/ lack of plasticity. Dollah et al.⁴ pointed out that enzymatic inter-esterification (EIE) of MOSO with palm stearin (PS) added to palm kernel oil (PKO) could yield fat molecules with better and harder biochemical frame-works that may contain desirable food grade nutritional and physical properties.⁴

So far 13 species have been reported from genus *Moringa*. MO is native to India, however, cultivated all over the world. MO is deciduous, with brittle stem, whitish-gray bark; leaves - pale green in color, bipinnate/ tri-pinnate with opposite, ovate leaflets. All plant parts of MO are endowed with nutraceutical/ pharmaceutical properties. MO has been traditionally used in various indigenous traditional systems of medicine (ITSM) as it is endowed with antioxidants, anti-diabetic, anti-bacterial, anti-fungal, anti-carcinogenic properties however, without side effects. Recently, MO has been considered for the development of Ready to Eat Functional Food Products, Food Grade Nutraceutical Products and therapeutic agents as like other medicinal plants⁵⁻³¹.

Pharmacological studies indicate that extracts obtained from MO have significant medicinal properties in relation to health and disease, but there isn't enough information on SA. ADMETox information on effects of SA is parsimoniously available, therefore, in the present study ADMETox profile of SA from MO has been carried out. Furthermore, DMPK properties of MO have been "fine-tuned" in order to expand the chances of making SA an apt candidate for clinical trials and biomedical applications.

MATERIALS AND METHODS

In silico Drug-Likelihood and Bioactivity Prediction

Drug likeliness and bioactivity of selected molecule was analyzed using Molinspiration server (<http://www.molinspiration.com>). Molinspiration tool is cheminformatics software that provides molecular properties as well as bioactivity prediction of compounds. In Molinspiration-based drug-likeness analysis, there are two important factors, including lipophilicity level (log P) and polar surface area (PSA) directly associated with pharmacokinetic properties (PK) of the compounds³². In Molinspiration-based bioactivity analysis, calculation of

bioactivity score of compounds toward GPCR ligands, ion channel modulators, kinase inhibitors, nuclear receptor ligands, protease inhibitors, and other enzyme targets were analyzed by Bayesian statistics³³. The analysis was carried out for G protein-coupled receptors (GPCR)³⁴, ion channels, kinases, nuclear hormone receptors, proteases, and other enzymes as major drug targets of SA

In silico ADMET Analysis

SwissADME is a Web tool that gives free access to a pool of fast yet robust predictive models for physicochemical properties, pharmacokinetics, druglikeness and medicinal chemistry friendliness, among which in-house proficient methods such as iLOGP (a physics-based model for lipophilicity) or BOILED-Egg.³⁵ PK properties, such as Absorption, Distribution, Metabolism, Excretion, and Toxicity (ADMET), of SA was predicted using admerSAR v2.0 server (<http://lmmd.ecust.edu.cn/admetSar2/>). admerSAR server is an open-source computational tool for prediction of ADMET properties of compounds, which makes it a practical platform for drug discovery and other pharmacological research. In ADMET analysis, absorption (A) of good drugs depends on factors such as membrane permeability [colon cancer cell line (Caco-2)]³⁶, human intestinal absorption (HIA)³⁷, and status of either P-glycoprotein substrate/ inhibitor³⁸. Distribution (D) of drugs mainly depends on the ability to cross blood-brain barrier (BBB)³⁹. Metabolism (M) of drugs is calculated by the CYP, MATE1, and OATP1B1-OATP1B3 models⁴⁰. Excretion (E) of drugs is estimated based on renal OCT substrate. Toxicity (T) of drugs is predicted on human ether-a-Go-Go related gene inhibition, carcinogenic status, mutagenic status, and acute oral toxicity^{41,42}.

vNN model building and analysis

vNN method was used to calculate the similarity distance between molecules in terms of their structure, and uses a distance threshold to define a domain of applicability to ensure that the predictions generated are reliable⁴³. vNN models can be built keeping quantitative structure-activity relationship (QSAR) models up-to-date to maintain their performance levels⁴⁴. Performance characteristics of the models are comparable, and often superior to those of other more elaborate model.¹⁵⁻¹⁸ One of the most widely used measures of similarity distance between two small molecules is Tanimoto distance, *d*, which is defined as:

$$d = 1 - \frac{n(P \cap Q)}{n(P) + n(Q) - (P \cap Q)}$$

where $n(P \cap Q)$ is number of features common to molecules *p* and *q*, and $n(P)$ and $n(Q)$ are the total numbers of features for molecules *p* and *q*, respectively. The predicted biological activity *y* is given by a weighted across structurally similar neighbours:

$$y = \frac{\sum_{i=1}^v y_i e^{-(d_i/h)^2}}{\sum_{i=1}^v e^{-(d_i/h)^2}} \quad d_i \leq d_0$$

where d_i denotes Tanimoto distance between a query molecule for which a prediction is made and a molecule *i* of the training set; d_0 is a Tanimoto-distance threshold, beyond which two molecules are no longer considered to be sufficiently similar to be included in the average; y_i is the experimentally measured activity of molecule *i*; *v* denotes the total number of molecules in the training set that satisfies the condition $d_i \leq d_0$; and *h* is a smoothing factor, which dampens the distance penalty. Values of *h* and d_0 are determined from cross-validation studies. To identify structurally similar

compounds, Accelrys extended-connectivity fingerprints with a diameter of four chemical bonds (ECFP4) was used.

Model Validation

A 10-fold cross-validation (CV) procedure was used to validate new models and to determine the values of smoothing factor h and Tanimoto distance d_0 . In this procedure, data was randomly divided into 10 sets, and used 9 to develop the model and 10th to validate it, this process was repeated 10 times, leaving each set of molecules out once.

Performance Measures

Following metrics were used to assess model performance. (1) sensitivity measures a model's ability to correctly detect true positives, (2) specificity measures a model's ability to detect true negatives, (3) accuracy measures a model's ability to make correct predictions and (4) kappa compares the probability of correct predictions to the probability of correct predictions by chance (its value ranges from +1 (perfect agreement between model prediction and experiment) to -1 (complete disagreement), with 0 indicating no agreement beyond that expected by chance).

$$\text{sensitivity} = \frac{TP}{TP + FN}$$

$$\text{specificity} = \frac{TN}{FP + TN}$$

$$\text{accuracy} = \frac{TP + TN}{TP + TN + FP + FN}$$

$$\text{kappa} = \frac{\text{accuracy} - \text{Pr}(e)}{1 - \text{Pr}(e)}$$

where TP, TN, FP, and FN denote the numbers of true positives, true negatives, false positives, and false negatives, respectively. Kappa is a metric for assessing the quality of binary classifiers. Pr (e) is an estimate of the probability of a correct prediction by chance. It is calculated as:

$$\text{Pr}(e) = \frac{(TP + FN)(TP + FP) + (TP + FN)(TP + FP)}{(TP + FN + FP + TN)^2}$$

The coverage is the proportion of test molecules with at least one nearest neighbour that meets the similarity criterion. The coverage is a measure of how many test compounds are within the applicability domain of a prediction model.

RESULTS AND DISCUSSION

SA is a saturated long-chain fatty acid with an 18-carbon backbone. SA is a major component of cocoa butter and shea butter. SA is a white solid with a mild odour, floats on water. SA is a saturated fatty acid present in animal and vegetable fats and oils. It is a waxy solid.

Chemical Kingdom	: Organic Compounds
Super Class	: Lipids and Lipid-like Molecules
Class	: Fatty Acyls

Subclass	: Fatty Acids and Conjugates
IUPAC Name	: Octadecanoic Acid
Common Name	: Stearic Acid (SA)
Synonym	: Ethyl Palmitate;(-)Hydroxycitric Acid;(-)
Compound CID	: 5281
PubChem Identifier	: 12366
ChEBI Identifier	: 28842
CAS Identifier	: 5281
Molecular Formula	: C ₁₈ H ₃₆ O ₂
Molecular Weight	: 284.5g/mol
Canonical SMILES	: CCCCCCCCCCCCCCCCC(=O)O
InChIKey	: QIQXTHQIDYTFRH-UHFFFAOYSA-N

Drug-likeness properties of SA

Score from cLogP: 0.358 (cLogP = 5.581); Score from logS: 0.763 (logS = -3.826); Score from molecular weight: 0.956 (molecular weight 242.0); Score from drug-likeness: 0.0 (drug-likeness = 35.364); No Risk of Mutagenicity Score = 1.0; No Risk of Tumorigenicity Score = 1.0; No Risk of Irritating Effects Score = 1.0; No Risk of Reproductive Effects Score = 1.0 respectively were predicted and the overall predicted drug score for compound 3 was calculated as 0.293.

Bio-molecular properties of SA

Calculated value for molecular properties of compound 1 were (values given in parenthesis) - mLogP (5.35); TPSA (26.30); Natoms (15); MW (214.35); nON (2); nOHNH (0); Nviolations (1); Nrotb (11); volume (214.74) respectively; and the calculated bioactivity scores for biological properties were - GPCR ligand³⁴ (-0.41); Ion channel modulator (-0.13); Kinase inhibitor (-0.73); Nuclear receptor ligand (-0.43); Protease inhibitor (-0.46); Enzyme inhibitor (-0.11) respectively (**Table 1**).

Physicochemical Properties of SA

Molecular Formula of SA = C₁₈H₃₆O₂; Molecular weight of SA = 284.48 g/mol; Number of heavy atoms in SA = 20; Number of aromatic heavy atoms = 0; Fraction Csp3 in SA = 0.94; Number of rotatable bonds in SA = 16; Number of H-bond acceptors in SA = 2; Number of H-bond donors in SA = 1; Molar Refractivity of SA = 90.41; TPSA of SA = 37.30 Å²; Lipophilicity properties of SA = -; Log Po/w (iLOGP) = 4.30; Log Po/w (XLOGP3) = 8.23; Log Po/w (WLOGP) = 6.33; Log Po/w (MLOGP) = 4.67; Log Po/w (SILICOS-IT) = 6.13; Consensus Log Po/w = 5.93; Water Solubility properties of SA - Log S (ESOL) = -5.73; Solubility = 5.26e-04 mg/ml; 1.85e-06 mol/l; Class = Moderately soluble; Log S (Ali) = -8.87; Solubility = 3.80e-07 mg/ml; 1.33e-09 mol/l; Class = Poorly soluble; Log S (SILICOS-IT) = -6.11; Solubility = 2.19e-04 mg/ml; 7.71e-07 mol/l; Class = Poorly soluble; Pharmacokinetics properties of SA - GI absorption of SA is High BBB permeant = No; P-gp substrate = No; CYP1A2 inhibitor = Yes; CYP2C19 inhibitor = No; CYP2C9 inhibitor = No; CYP2D6 inhibitor = No; CYP3A4 inhibitor = No; Log Kp (skin permeation) = -2.19 cm/s; Druglikeness properties of SA - Lipinski's Rule for SA is Yes; (1 violation: MLOGP>4.15); Ghose's Rule for SA is No; (1 violation: WLOGP>5.6); Veber's Rule for SA is No; (1 violation:

Rotors>10); Egan Rule for SA is No; (1 violation: WLOGP>5.88); Muegge's Rule for SA is No;(2 violations: XLOGP3>5, Rotors>15); Bioavailability Score for SA = 0.85 Fig. 1; Medicinal Chemistry properties of SA - PAINS for SA is 0; Brenk's for SA is No; Leadlikeness for SA is No; (2 violations: Rotors>7, XLOGP3>3.5); Accessibility for SA = 2.54. Percentage distribution of function targets for SA using Swiss Target Prediction is given in Fig. 2; Table 2. Predicted ADMET Properties of SA is given in Table 3 and the summative

physicochemical, druggable, ADMET properties of SA have been provided in Table 4.

vNN model based ADMET analysis of SA

Implemented Absorption, Distribution, Metabolism, Excretion and Toxicity (ADMET) prediction models, including their performance measures has been carried out. Model covers diverse set of ADMET endpoints for Maximum Recommended Therapeutic Dose (MRTD), mutagenicity, human liver microsomal (HLM), Pgp inhibitor/substrates (Table 5).

Query	Liver Toxicity		Metabolism						Membrane Transporters			Others			
	DILI	Cytotoxicity	HLM	Cyp Inhibitors for					BBB	P-gp Inhibitor	P-gp Substrate	hERG Blocker	MMP	AMES	MRTD (mg/day)
				1A2	3A4	2D6	2C9	2C19							
	Yes	No	No	No	No	No	No	No	No	No	No	Yes	No	No	20

Liver Toxicity

Drug-induced liver injury (DILI) has been one of the most common reasons for drug withdrawal from market. This application predicts whether a compound could cause DILI. A dataset of 1,431 compounds was obtained from online sources. Dataset contained both pharmaceuticals and non-pharmaceuticals; a compound was classified as causing DILI if it was associated with a high risk of DILI and not if there was no such risk⁴⁵ that includes SA (Table 5).

Cytotoxicity (HepG2)

Cytotoxicity is the degree to which a chemical causes damage to cells. A cytotoxicity prediction model was developed using in vitro data on toxicity against HepG2 cells for 6,000 structurally diverse compounds, including SA were collected from ChEMBL. In developing the model, the compounds with an $IC_{50} \leq 10 \mu M$ were considered in the in vitro assay as cytotoxic (Table 5).

Metabolism - HLM

Human Liver Microsomal (HLM) stability assay is commonly used to identify and exclude compounds that are too rapidly metabolized. For a drug to achieve effective therapeutic concentrations in the body, it cannot be metabolized too rapidly by the liver. Compounds with a half-life of 30 min or longer in an HLM assay were considered as stable; otherwise unstable. HLM data was retrieved from ChEMBL database, manually curated and classified compounds as stable or unstable based on reported half-life ($T_{1/2} > 30$ min was considered stable, and $T_{1/2} < 30$ min unstable). The final dataset contained 3,654 compounds. Of these, as much as 2,313 including SA were classified as stable and 1,341 as unstable (Table 5).

Cytochrome P450 enzyme (CYP) inhibition

CYPs play an important role in metabolism and detoxification of xenobiotics. In vitro data derived from five main drug-metabolizing CYPs-1A2, 3A4, 2D6, 2C9 and 2C19 was used to develop CYP inhibition models. CYP inhibitors were retrieved from PubChem and classified a compound with an $IC_{50} \leq 10 \mu M$ for an enzyme as an inhibitor of the enzyme. Predictions for the following enzymes: CYP1A2, CYP3A4, CYP2D6, CYP2C9, and CYP2C19 have been provided for SA in Table 5.

Membrane Transporters - Blood-Brain Barrier (BBB)

BBB is a highly selective barrier that separates the circulating blood from the central nervous system⁴⁶. VNN-based BBB

model has been developed, using 352 compounds whose BBB permeability values ($\log_{10}BBB$) were obtained from the literature Compounds with $\log BBB$ values of less than -0.3 and greater than +0.3 were classified as BBB non-permeable and permeable. Calculated BBB value of SA is **-0.195** based on WLOGP vs TPSA using BOILED-Egg Fig. 3; Table 5.

Pgp Substrates/ Inhibitors

P-glycoprotein (Pgp) is an essential cell membrane protein that extracts many foreign substances from the cell. Cancer cells often overexpress Pgp, which increases the efflux of chemotherapeutic agents from the cell and prevents treatment by reducing the effective intracellular concentrations known as multidrug resistance. For this reason, identifying compounds that can either be transported out of the cell by Pgp (substrates) or impair Pgp function (inhibitors) is required. Models to predict both Pgp substrates and Pgp inhibitors were developed. Pgp substrate dataset consists of measurements of 422 substrates and 400 non-substrates. To generate a large Pgp inhibitor dataset, both the datasets were combined and duplicates were removed to form a combined dataset consisting of a training set of 1,319 inhibitors and 937 non-inhibitors. Analysis indicates that SA is neither a P-glycoprotein substrate nor P-glycoprotein I/II inhibitor as indicated⁴⁷ (Table 5).

hERG (Cardiotoxicity):

human ether-à-go-go-related gene (hERG) codes for a potassium ion channel involved in the normal cardiac repolarization activity of the heart. Drug-induced blockade of hERG function can cause long QT syndrome, which may result in arrhythmia and death⁴⁸. As much as 282 known hERG blockers from the literature were retrieved and classified compounds with an IC_{50} cut-off value of $10 \mu M$ or less as blockers. A set of 404 compounds with IC_{50} values greater than $10 \mu M$ were classified as non-blockers. Prediction indicated SA as hERG I non - inhibitor and hERG II as non - inhibitor (Table 5).

MMP (Mitochondrial Toxicity)

Fundamental role of mitochondria in cellular energetics and oxidative stress, mitochondrial dysfunction has been implicated in cancer, diabetes, neurodegenerative disorders, and cardiovascular diseases. A largest dataset of chemical-induced changes in mitochondrial membrane potential (MMP), was used based on the assumption that a compound that causes mitochondrial dysfunction is also likely to reduce the MMP. vNN-based MMP prediction model was developed using

6,261 compounds collected from a previous study that screened a library of more than 10,000 compounds (~8,300 unique chemicals) at 15 concentrations, each in triplicate, to measure changes in the MMP in HepG2 cells. The study found that 913 compounds decreased the MMP, whereas 5,395 compounds had no effect (Table 5). SA was predicted to be Non-carcinogens with a calculated value of 0.575.

Mutagenicity (Ames test)

Mutagens are chemicals that cause abnormal genetic mutations leading to cancer. A common way to assess a chemical's mutagenicity is the Ames test. A prediction model was developed using a literature dataset of 6,512 compounds, of which 3,503 were Ames-positive. Prediction indicated SA as Non AMES toxic with a calculated value of 0.963 (Table 5).

Maximum Recommended Therapeutic Dose (MRTD)

MRTD is an estimated upper daily dose that is considered to be safe. A prediction model was developed based on a dataset of MRTD values disclosed by the FDA, mostly of single-day oral doses for an average adult with a body weight of 60 kg, for 1,220 compounds (small organic drugs). Organometallics, high-molecular weight polymers were excluded (>5,000 Da), nonorganic chemicals, mixtures of chemicals, and very small molecules (<100 Da). An external test set of 160 compounds collected by FDA was used for validation. The total dataset for the model contained 1,185 compounds⁴⁹. The predicted MRTD value is reported in mg/day unit based upon an average adult weighing 60 kg. MRTD for SA was calculated as -0.791 (Table 5).

CONCLUSION

ADMET-informatics of Octadecanoic Acid (Stearic Acid) from ethyl acetate fraction of *Moringa oleifera* leaves has been envisaged to predict drug metabolism and pharmacokinetics (DMPK) outcomes. ADMET informatics contributes to the deeper understanding of SA as a major source of drug lead from *Moringa oleifera* with immense therapeutic potential. Results indicate that SA is of GRAS standard drug with predicted values within the range suitable for human consumption. Data generated herein could be useful for the development of SA as PBNPL for next generation drug design, development and therapies.

REFERENCES

- Acid L. Final report on the safety assessment of oleic acid, lauric acid, palmitic acid, myristic acid, and stearic acid. *J. Am. Coll. Toxicol.* 1987; 6:321-401. <https://doi.org/10.3109/10915818709098563>
- Meyer F, Bloch K. Metabolism of stearic acid in yeast. *Journal of Biological Chemistry.* 1963 Aug 1; 238(8):2654-9. [https://doi.org/10.1016/S0021-9258\(18\)67881-0](https://doi.org/10.1016/S0021-9258(18)67881-0)
- Warra AA, Jonathan BL, Ibrahim BD, Adedara AO. GC-MS Analysis of Hexane Extracts of Two Varieties of Sesame (*Sesamum indicum* L.) Seed Oil. *IJCPT* 2016; 1(1):1-9
- Dollah S, Abdulkarim SM, Ahmad SH, Khoramnia A, Mohd Ghazali H. Physico-chemical properties of *Moringa oleifera* seed oil enzymatically inter-esterified with palm stearin and palm kernel oil and its potential application in food. *Journal of the Science of Food and Agriculture.* 2016 Aug; 96(10):3321-33. <https://doi.org/10.1002/jsfa.7510>
- Ramya S, Neethirajan K, Jayakumararaj R. Profile of bioactive compounds in *Syzygium cumini*-a review. *Journal of Pharmacy Research.* 2012; 5(8):4548-53.
- Kandeepan C, Sukanandam K, Jeevalatha A, Kavitha N, Senthilkumar N, Sutha S, Syed MA, Gandhi S, Ramya S, Grace Lydial Pushpalatha G, Abraham GC, King Immanuel J, Jayakumararaj R, ADMETE valuation, Pharmacokinetics, Drug-likeness and Medicinal Chemistry of GCMS Identified Bioactive Compounds of *Moringa oleifera* Natural-Ripened Dried Methanolic Pod Extract (MOMPE) as a Potential Source of Natural Drug Frontrunner for Next Generation Drug Design, Development and Therapeutics. *Journal of Drug Delivery and Therapeutics.* 2022; 12(6):65-85 <https://doi.org/10.22270/jddt.v12i5-S.5657>
- Ramya S, Chandran M, King IJ, Jayakumararaj R, Loganathan T, Pandiarajan G, Kaliraj P, Grace Lydial Pushpalatha G, Abraham GC, Vijaya V., Aruna D, Sutha S, Dhakar RC, Phytochemical Screening, GCMS and FTIR Profile of Bioactive Compounds in *Solanum lycopersicum* Wild Fruits collected from Palani Hill Ranges of the Western Ghats, *Journal of Drug Delivery and Therapeutics.* 2022; 12(6):56-64 <https://doi.org/10.22270/jddt.v12i2-S.5280>
- Chandran M, Priyanka R, Kavipriya D, Ramya S, Jayakumararaj R, Loganathan T, Pandiarajan G, Kaliraj P, Pushpalatha GG, Abraham GC, Dhakar RC. Reformulation and Scientific Evaluation of CUSOCO: A Traditional Toothpaste Formula from Classical Tamil Literature towards treatment of Halitosis. *Journal of Drug Delivery and Therapeutics.* 2022; 12(5):127-31. <https://doi.org/10.22270/jddt.v12i5.5604>
- Kalaimathi RV, Krishnaveni K, Murugan M, Basha AN, Gilles AP, Kandeepan C, Senthilkumar N, Mathialagan B, Ramya S, Ramanathan L, Jayakumararaj R. ADMET informatics of Tetradecanoic acid (Myristic Acid) from ethyl acetate fraction of *Moringa oleifera* leaves. *Journal of Drug Delivery and Therapeutics.* 2022; 12(4-S):101-11. <https://doi.org/10.22270/jddt.v12i4-S.5533>
- Nazar S, Jayaseelan M, Jayakumararaj R. Local Health Traditions, Cultural Reflections and Ethno-taxonomical Information on Wild Edible Fruit Yielding Medicinal Plants in Melur Region of Madurai District, TamilNadu, India. *Journal of Drug Delivery and Therapeutics.* 2022; 12(3):138-57. <https://doi.org/10.22270/jddt.v12i3.5405>
- Murugan M, Krishnaveni K, Sabitha M, Kandeepan C, Senthilkumar N, Loganathan T, Pushpalatha GL, Pandiarajan G, Ramya S, Jayakumararaj R. In silico Target Class Prediction and Probabilities for Plant Derived Omega 3 Fatty Acid from Ethyl Acetate Fraction of *Moringa oleifera* Leaf Extract. *Journal of Drug Delivery and Therapeutics.* 2022; 12(3):124-37. <https://doi.org/10.22270/jddt.v12i3.5352>
- Parvathi K, Kandeepan C, Sabitha M, Senthilkumar N, Ramya S, Boopathi NM, Ramanathan L, Jayakumararaj R. In-silico Absorption, Distribution, Metabolism, Elimination and Toxicity profile of 9, 12, 15-Octadecatrienoic acid (ODA) from *Moringa oleifera*. *Journal of Drug Delivery and Therapeutics.* 2022; 12(2-S):142-50. <https://doi.org/10.22270/jddt.v12i2-S.5289>
- Ramya S, Loganathan T, Chandran M, Priyanka R, Kavipriya K, Pushpalatha GG, Aruna D, Ramanathan L, Jayakumararaj R, Saluja V. Phytochemical Screening, GCMS, FTIR profile of Bioactive Natural Products in the methanolic extracts of *Cuminum cyminum* seeds and oil. *Journal of Drug Delivery and Therapeutics.* 2022; 12(2-S):110-8. <https://doi.org/10.22270/jddt.v12i2-S.5280>
- Kandeepan C, Sabitha M, Parvathi K, Senthilkumar N, Ramya S, Boopathi NM, Jayakumararaj R. Phytochemical Screening, GCMS Profile, and In-silico properties of Bioactive Compounds in Methanolic Leaf Extracts of *Moringa oleifera*. *Journal of Drug Delivery and Therapeutics.* 2022; 12(2):87-99. <https://doi.org/10.22270/jddt.v12i2.5250>
- Krishnaveni K, Sabitha M, Murugan M, Kandeepan C, Ramya S, Loganathan T, Jayakumararaj R. vNN model cross validation towards Accuracy, Sensitivity, Specificity and kappa performance measures of β -caryophyllene using a restricted-unrestricted applicability domain on Artificial Intelligence & Machine Learning approach based in-silico prediction. *Journal of Drug Delivery and Therapeutics.* 2022; 12(1-S):123-31. <https://doi.org/10.22270/jddt.v12i1-S.5222>
- Jeevalatha A, Kalaimathi RV, Basha AN, Kandeepan C, Ramya S, Loganathan T, Jayakumararaj R. Profile of bioactive compounds in

- Rosmarinus officinalis. Journal of Drug Delivery and Therapeutics. 2022; 12(1):114-22. <https://doi.org/10.22270/jddt.v12i1.5189>
17. Kalaimathi RV, Jeevalatha A, Basha AN, Kandeepan C, Ramya S, Loganathan T, Jayakumararaj R. In-silico Absorption, Distribution, Metabolism, Elimination and Toxicity profile of Isopulegol from Rosmarinus officinalis. Journal of Drug Delivery and Therapeutics. 2022; 12(1):102-8. <https://doi.org/10.22270/jddt.v12i1.5188>
18. Ramya S, Loganathan T, Chandran M, Priyanka R, Kavipriya K, Pushpalatha GL, Aruna D, Abraham GC, Jayakumararaj R. ADME-Tox profile of Cuminaldehyde (4-Isopropylbenzaldehyde) from Cuminum cyminum seeds for potential biomedical applications. Journal of Drug Delivery and Therapeutics. 2022; 12(2-S):127-41. <https://doi.org/10.22270/jddt.v12i2-S.5286>
19. Ramya S, Murugan M, Krishnaveni K, Sabitha M, Kandeepan C, Jayakumararaj R. In-silico ADMET profile of Ellagic Acid from Syzygium cumini: A Natural Biaryl Polyphenol with Therapeutic Potential to Overcome Diabetic Associated Vascular Complications. Journal of Drug Delivery and Therapeutics. 2022; 12(1):91-101. <https://doi.org/10.22270/jddt.v12i1.5179>
20. Ramya S, Soorya C, Pushpalatha GG, Aruna D, Loganathan T, Balamurugan S, Abraham GC, Ponrathy T, Kandeepan C, Jayakumararaj R. Artificial Intelligence and Machine Learning approach based in-silico ADME-Tox and Pharmacokinetic Profile of α -Linolenic acid from Catharanthus roseus (L.) G. Don. Journal of Drug Delivery and Therapeutics. 2022; 12(2-S):96-109. <https://doi.org/10.22270/jddt.v12i2-S.5274>
21. Ramya S, Sutha S, Chandran M, Priyanka R, Loganathan T, Pandiarajan G, Kaliraj P, Grace Lydial Pushpalatha G, Abraham GC, Jayakumararaj R, ADMET-informatics, Pharmacokinetics, Drug-likeness and Medicinal Chemistry of Bioactive Compounds of Physalis minima Ethanolic Leaf Extract (PMELE) as a Potential Source of Natural Lead Molecules for Next Generation Drug Design, Development and Therapies, Journal of Drug Delivery and Therapeutics. 2022; 12(5):188-200 <https://doi.org/10.22270/jddt.v12i5.5654>
22. Suganandam K, Jeevalatha A, Kandeepan C, Kavitha N, Senthilkumar N, Sutha S, Syed MA, Gandhi S, Ramya S, Grace Lydial Pushpalatha G, Abraham GC, Jayakumararaj R, Profile of Phytochemicals and GCMS Analysis of Bioactive Compounds in Natural Dried-Seed Removed Ripened Pods Methanolic Extracts of Moringa oleifera, Journal of Drug Delivery and Therapeutics. 2022; 12(5-S):133-141 <https://doi.org/10.22270/jddt.v12i5-S.5657>
23. Kandeepan C, Kalaimathi RV, Jeevalatha A, Basha AN, Ramya S, Jayakumararaj R. In-silico ADMET Pharmacoinformatics of Geraniol (3, 7-dimethylocta-trans-2, 6-dien-1-ol)-acyclic monoterpene alcohol drug from Leaf Essential Oil of Cymbopogon martinii from Sirumalai Hills (Eastern Ghats), INDIA. Journal of Drug Delivery and Therapeutics. 2021; 11(4-S):109-18. <https://doi.org/10.22270/jddt.v11i4-S.4965>
24. Loganathan T, Barathinivas A, Soorya C, Balamurugan S, Nagajothi TG, Ramya S, Jayakumararaj R. Physicochemical, Druggable, ADMET Pharmacoinformatics and Therapeutic Potentials of Azadirachtin-a Prenol Lipid (Triterpenoid) from Seed Oil Extracts of Azadirachta indica A. Juss. Journal of Drug Delivery and Therapeutics. 2021; 11(5):33-46. <https://doi.org/10.22270/jddt.v11i5.4981>
25. Sabitha M, Krishnaveni K, Murugan M, Basha AN, Pallan GA, Kandeepan C, Ramya S, Jayakumararaj R. In-silico ADMET predicated Pharmacoinformatics of Quercetin-3-Galactoside, polyphenolic compound from Azadirachta indica, a sacred tree from Hill Temple in Alagarkovil Reserve Forest, Eastern Ghats, INDIA. Journal of Drug Delivery and Therapeutics. 2021; 11(5-S):77-84. <https://doi.org/10.22270/jddt.v11i5-S.5026>
26. Soorya C, Balamurugan S, Basha AN, Kandeepan C, Ramya S, Jayakumararaj R. Profile of Bioactive Phyto-compounds in Essential Oil of Cymbopogon martinii from Palani Hills, Western Ghats, INDIA. Journal of Drug Delivery and Therapeutics. 2021; 11(4):60-5. <https://doi.org/10.22270/jddt.v11i4.4887>
27. Soorya C, Balamurugan S, Ramya S, Neethirajan K, Kandeepan C, Jayakumararaj R. Physicochemical, ADMET and Druggable properties of Myricetin: A Key Flavonoid in Syzygium cumini that regulates metabolic inflammations. Journal of Drug Delivery and Therapeutics. 2021; 11(4):66-73. <https://doi.org/10.22270/jddt.v11i4.4890>
28. Shanmugam S, Sundari A, Muneeswaran S, Vasanth C, Jayakumararaj R, Rajendran K. Ethnobotanical Indices on medicinal plants used to treat poisonous bites in Thiruppuvanam region of Sivagangai district in Tamil Nadu, India. Journal of Drug Delivery and Therapeutics. 2020; 10(6-s):31-6. <https://doi.org/10.22270/jddt.v10i6-s.4432>
29. Sundari A, Jayakumararaj R. Herbal remedies used to treat skin disorders in Arasankulam region of Thoothukudi District in Tamil Nadu, India. Journal of Drug Delivery and Therapeutics. 2020; 10(5):33-8. <https://doi.org/10.22270/jddt.v10i5.4277>
30. Sundari A, Jayakumararaj R. Medicinal plants used to cure cuts and wounds in Athur region of Thoothukudi district in Tamil Nadu, India. Journal of Drug Delivery and Therapeutics. 2020; 10(6-s):26-30. <https://doi.org/10.22270/jddt.v10i6-s.4429>
31. Meena R, Prajapati SK, Nagar R, Porwal O, Nagar T, Tilak VK, Jayakumararaj R, Arya RK, Dhakar RC. Application of Moringa oleifera in Dentistry. Asian Journal of Dental and Health Sciences. 2021; 1(1):10-3. <https://doi.org/10.22270/ijmspr.v6i1.25>
32. Beetge E, du Plessis J, Müller DG, Goosen C, van Rensburg FJ. The influence of the physicochemical characteristics and pharmacokinetic properties of selected NSAID's on their transdermal absorption. International Journal of Pharmaceutics. 2000; 193(2):261-4. [https://doi.org/10.1016/S0378-5173\(99\)00340-3](https://doi.org/10.1016/S0378-5173(99)00340-3)
33. Mabkhot YN, Alatibi F, El-Sayed NN, Al-Showiman S, Kheder NA, Wadood A, Rauf A, Bawazeer S, Hadda TB. Antimicrobial activity of some novel armed thiophene derivatives and petra/osisiris/molinspiration (POM) analyses. Molecules. 2016; 21(2):222. <https://doi.org/10.3390/molecules21020222>
34. Hauser AS, Attwood MM, Rask-Andersen M, Schiöth HB, Gloriam DE. Trends in GPCR drug discovery: new agents, targets and indications. Nature reviews Drug discovery. 2017 Dec; 16(12):829-42. <https://doi.org/10.1038/nrd.2017.178>
35. Daina A, Michielin O, Zoete V. SwissADME: a free web tool to evaluate pharmacokinetics, drug-likeness and medicinal chemistry friendliness of small molecules. Scientific reports. 2017; 7(1):1-3 <https://doi.org/10.1038/srep42717>
36. Hubatsch I, Ragnarsson EG, Artursson P. Determination of drug permeability and prediction of drug absorption in Caco-2 monolayers. Nature protocols. 2007; 2(9):2111-9. <https://doi.org/10.1038/nprot.2007.303>
37. Radchenko EV, Dyabina AS, Palyulin VA, Zefirov NS. Prediction of human intestinal absorption of drug compounds. Russian Chemical Bulletin. 2016; 65(2):576-80. <https://doi.org/10.1007/s11172-016-1340-0>
38. Alam A, Kowal J, Broude E, Roninson I, Locher KP. Structural insight into substrate and inhibitor discrimination by human Pglycoprotein. Science. 2019; 363(6428):753-6. <https://doi.org/10.1126/science.aav7102>
39. Daina A, Zoete V. A boiled-egg to predict gastrointestinal absorption and brain penetration of small molecules. ChemMedChem. 2016; 11(11):1117-21. <https://doi.org/10.1002/cmdc.201600182>
40. Liao M, Jaw-Tsai S, Beltman J, Simmons AD, Harding TC, Xiao JJ. Evaluation of in vitro absorption, distribution, metabolism, and excretion and assessment of drug-drug interaction of rucaparib, an orally potent poly (ADP-ribose) polymerase inhibitor. Xenobiotica. 2020; 50(9):1032-42. <https://doi.org/10.1080/00498254.2020.1737759>
41. Jia CY, Li JY, Hao GF, Yang GF. A drug-likeness toolbox facilitates ADMET study in drug discovery. Drug Discovery Today. 2020; 25(1):248-58. <https://doi.org/10.1016/j.drudis.2019.10.014>

42. Cheng F, Li W, Zhou Y, Shen J, Wu Z, Liu G, Lee PW, Tang Y. admetSAR: a comprehensive source and free tool for assessment of chemical ADMET properties.
43. Schyman, P., R. Liu, V. Desai, and A. Wallqvist. vNN web server for ADMET predictions. *Frontiers in Pharmacology*. 2017 December 4; 8:889. <https://doi.org/10.3389/fphar.2017.00889>
44. Liu, R., P. Schyman, and A. Wallqvist. Critically assessing the predictive power of QSAR models for human liver microsomal stability. *Journal of Chemical Information and Modeling*. 2015; 55(8):1566-1575. <https://doi.org/10.1021/acs.jcim.5b00255>
45. Xu, Y., Z. Dai, F. Chen, S. Gao, J. Pei, and L. Lai. Deep learning for drug induced liver injury. 2015, 55(10):2085-2093. <https://doi.org/10.1021/acs.jcim.5b00238>
46. Muehlbacher, M., G. Spitzer, K. Liedl, J. Kornhuber. Qualitative prediction of blood-brain barrier permeability on a large and refined dataset. *Journal of Computer-Aided Molecular Design*. 2011; 25:1095. <https://doi.org/10.1007/s10822-011-9478-1>
47. Schyman, P., R. Liu, and A. Wallqvist. Using the variable-nearest neighbor method to identify P-glycoprotein substrates and inhibitors. *ACS Omega*. 2016; 1(5):923-929 <https://doi.org/10.1021/acsomega.6b00247>
48. Schyman, P., R. Liu, and A. Wallqvist. General purpose 2D and 3D similarity approach to identify hERG blockers. *Journal of Chemical Information and Modeling*. 2016; 56(1):213-222 <https://doi.org/10.1021/acs.jcim.5b00616>
49. Liu, R., G. Tawa, and A. Wallqvist. Locally weighted learning methods for predicting dose-dependent toxicity with application to the human maximum recommended daily dose. *Chemical Research in Toxicology*. 2012; 25(10):2216-2226. <https://doi.org/10.1021/tx300279f>

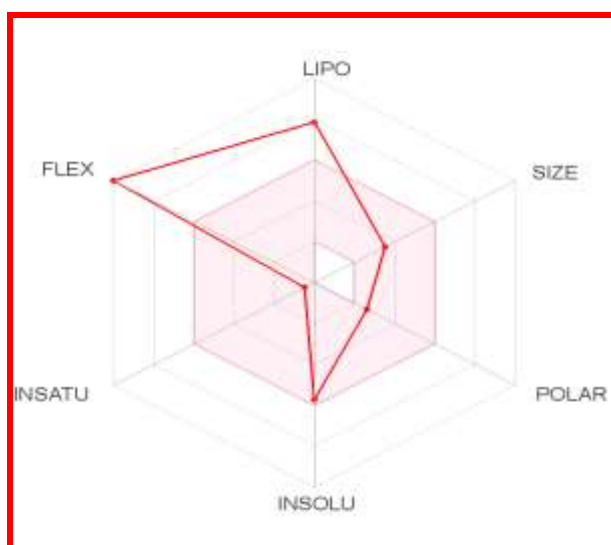


Figure 1: Schematic diagram of Bioavailability Radar for Drug likeness of SA (lipophilicity: $XLOGP3$ between -0.7 and +5.0, size: MW between 150 and 500 g/mol, polarity: TPSA between 20 and 130 Å², solubility: log S not higher than 6, saturation: fraction of carbons in the sp^3 hybridization not less than 0.25, and flexibility: no more than 9 rotatable bonds)

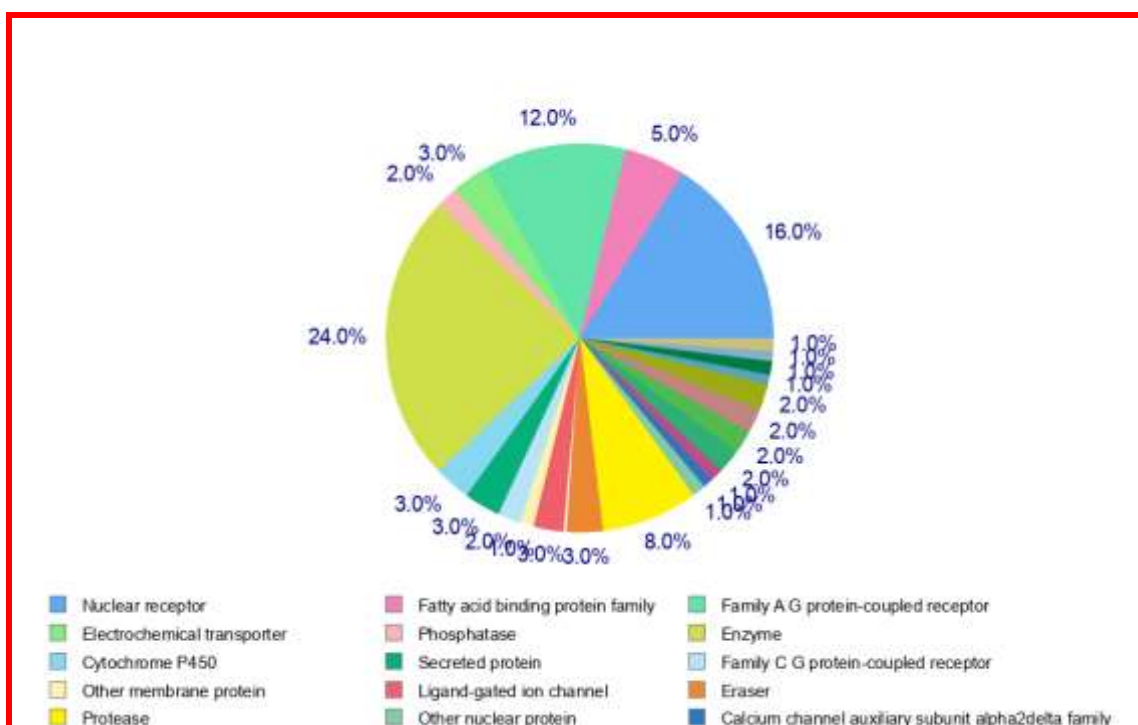


Figure 2: Percentage distribution of function targets for SA using SwissTargetPrediction

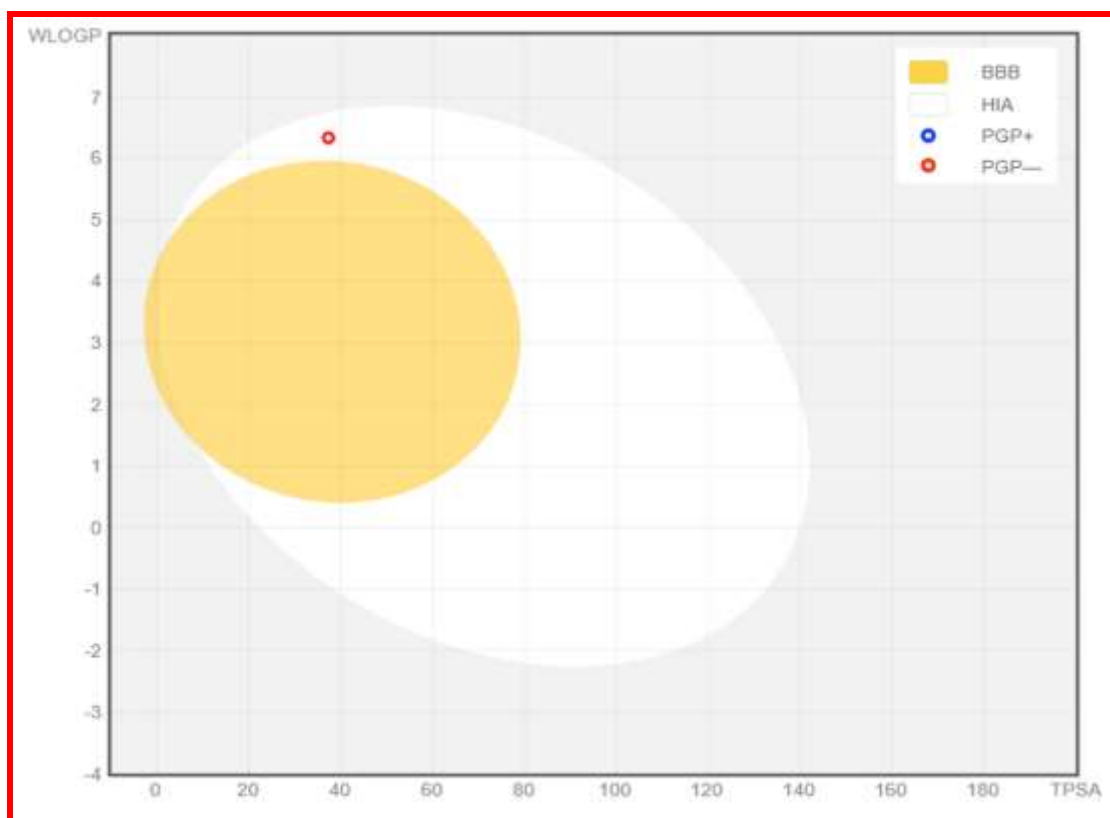


Figure 3: Schematic representation of perceptive evaluation of passive gastrointestinal absorption (HIA) and Brain penetration (BBB) of SA with WLOGP-versus-TPSA using BOILED-Egg

Table 1: *In silico* Drug-Likeliness and Bioactivity Prediction

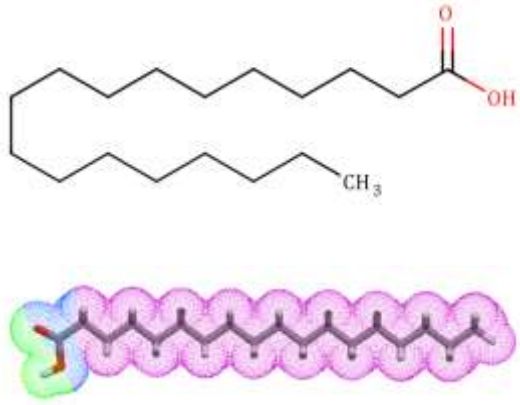
	Molecular Properties	Calculated Values
		miLogP
	TPSA	37.30
	Natoms	20
	MW	284.48
	nON	2
	nOHNH	1
	Nviolations	1
	Nrotb	16
	volume	325.03
	Biological Properties	Bioactivity Scores
	GPCR ligand	0.11
	Ion channel modulator	0.05
	Kinase inhibitor	-0.20
	Nuclear receptor ligand	0.17
	Protease inhibitor	0.06
	Enzyme inhibitor	0.20

Table 2: Predicted Target/ Target Class and Functional Probabilities of SA

TARGET	COMMON.NAME	UNIPROT.ID	TARGET CLASS	PROBABILITY*
Peroxisome proliferator-activated receptor alpha	PPARA	Q07869	Nuclear receptor	0.929299883958
Peroxisome proliferator-activated receptor delta	PPARD	Q03181	Nuclear receptor	0.929299883958
Fatty acid binding protein adipocyte	FABP4	P15090	Fatty acid BPF	0.714850037542
Fatty acid binding protein epidermal	FABP5	Q01469	Fatty acid BPF	0.714850037542
Fatty acid binding protein muscle	FABP3	P05413	Fatty acid BPF	0.526361274524
Fatty acid binding protein intestinal	FABP2	P12104	Fatty acid BPF	0.526361274524
Free fatty acid receptor 1	FFAR1	O14842	Family A GPCR	0.370888463379
Solute carrier family 22 member 6	SLC22A6	Q4U2R8	Electrochemical transporter	0.207053973629
Dual specificity phosphatase Cdc25A	CDC25A	P30304	Phosphatase	0.17427075329
Aldo-keto reductase family 1 member B10	AKR1B10	O60218	Enzyme	0.149732593856
11-beta-hydroxysteroid dehydrogenase 1	HSD11B1	P28845	Enzyme	0.149732593856
Bile acid receptor FXR	NR1H4	Q96R11	Nuclear receptor	0.125142648574
UDP-glucuronosyltransferase 2B7	UGT2B7	P16662	Enzyme	0.125142648574
Prostanoid EP2 receptor	PTGER2	P43116	Family A GPCR	0.125142648574
DNA polymerase beta	POLB	P06746	Enzyme	0.125142648574
Cytochrome P450 19A1	CYP19A1	P11511	Cytochrome P450	0.116965063224
Corticosteroid binding globulin	SERPINA6	P08185	Secreted protein	0.116965063224
Testis-specific androgen-binding protein	SHBG	P04278	Secreted protein	0.116965063224
Estradiol 17-beta-dehydrogenase 3	HSD17B3	P37058	Enzyme	0.116965063224
Glucose-6-phosphate 1-dehydrogenase	G6PD	P11413	Enzyme	0.116965063224
GABA-B receptor	GABBR1	Q9UBS5	Family C GPCR	0.116965063224
G-protein coupled bile acid receptor 1	GPBAR1	Q8TDU6	Family A GPCR	0.108770969359
Niemann-Pick C1-like protein 1	NPC1L1	Q9UHC9	Other membrane protein	0.108770969359
GABA A receptor alpha-2/beta-2/gamma-2	GABRA2	P47869	Ligand-gated ion channel	0.108770969359
Lysine-specific demethylase 2A	KDM2A	Q9Y2K7	Eraser	0.108770969359
Lysine-specific demethylase 5C	KDM5C	P41229	Eraser	0.108770969359
Vitamin D receptor	VDR	P11473	Nuclear receptor	0.108770969359
Androgen Receptor	AR	P10275	Nuclear receptor	0.100578902067
Protein farnesyltransferase	FNTA	P49354	Enzyme	0.100578902067
Histone lysine demethylase PHF8	PHF8	Q9UPP1	Eraser	0.100578902067
Plasminogen	PLG	P00747	Protease	0.100578902067
Glutathione S-transferase kappa 1	GSTK1	Q9Y2Q3	Enzyme	0.100578902067
Protein-tyrosine phosphatase 1B	PTPN1	P18031	Phosphatase	0.100578902067
Anandamide amidohydrolase	FAAH	O00519	Enzyme	0.100578902067
Peroxisome proliferator-activated receptor gamma	PPARG	P37231	Nuclear receptor	0.100578902067
Telomerase reverse transcriptase	TERT	O14746	Enzyme	0.100578902067

Fatty acid-binding protein, liver	FABP1	P07148	Fatty acid BPF	0.100578902067
Retinoic acid receptor gamma	RARG	P13631	Nuclear receptor	0.100578902067
Retinoic acid receptor beta	RARB	P10826	Nuclear receptor	0.100578902067
Retinoic acid receptor alpha	RARA	P10276	Nuclear receptor	0.100578902067
Glycine receptor subunit alpha-1	GLRA1	P23415	Ligand-gated ion channel	0.100578902067
11-beta-hydroxysteroid dehydrogenase 2	HSD11B2	P80365	Enzyme	0.100578902067
Prostanoid FP receptor	PTGFR	P43088	Family A GPCR	0.100578902067
CDC45-related protein	CDC45	O75419	Other nuclear protein	0.100578902067
Leukocyte common antigen	PTPRC	P08575	Enzyme	0.100578902067
Hydroxyacid oxidase 1	HAO1	Q9UJM8	Enzyme	0.100578902067
Nuclear receptor subfamily 0 group B member 2	NR0B2	Q15466	Nuclear receptor	0.100578902067
Cytochrome P450 26B1	CYP26B1	Q9NR63	Cytochrome P450	0.100578902067
Cytochrome P450 26A1	CYP26A1	O43174	Cytochrome P450	0.100578902067
Acyl-CoA desaturase	SCD	O00767	Enzyme	0.100578902067
Retinoid X receptor beta	RXRB	P28702	Nuclear receptor	0.100578902067
Retinoid X receptor gamma	RXRG	P48443	Nuclear receptor	0.100578902067
Retinoid X receptor alpha	RXRA	P19793	Nuclear receptor	0.100578902067
Voltage-gated calcium channel alpha2/delta subunit 1	CACNA2D1	P54289	Calcium channel	0.100578902067
HMG-CoA reductase	HMGCR	P04035	Oxidoreductase	0.100578902067
Prostanoid EP4 receptor	PTGER4	P35408	Family A GPCR	0.100578902067
Neuronal acetylcholine receptor protein alpha-7 subunit	CHRNA7	P36544	Ligand-gated ion channel	0.100578902067
Carbonic anhydrase II	CA2	P00918	Lyase	0.100578902067
Carbonic anhydrase I	CA1	P00915	Lyase	0.100578902067
Glucagon	GCG	P01275	Unclassified protein	0.100578902067
SUMO-activating enzyme	SAE1	Q9UBE0	Enzyme	0.100578902067
Metabotropic glutamate receptor 5	GRM5	P41594	Family C GPCR	0.100578902067
Phosphodiesterase 4A	PDE4A	P27815	Phosphodiesterase	0.100578902067
Phosphodiesterase 4B	PDE4B	Q07343	Phosphodiesterase	0.100578902067

Table 3: Predicted ADMET Properties of SA

Property	Model Name	Predicted Value	Unit
Absorption	Water solubility	-5.973	Numeric (log mol/L)
Absorption	Caco2 permeability	1.556	Numeric (log Papp in 10 ⁻⁶ cm/s)
Absorption	Intestinal absorption (human)	91.317	Numeric (% Absorbed)
Absorption	Skin Permeability	-2.726	Numeric (log Kp)
Absorption	P-glycoprotein substrate	No	Categorical (Yes/No)
Absorption	P-glycoprotein I inhibitor	No	Categorical (Yes/No)
Absorption	P-glycoprotein II inhibitor	No	Categorical (Yes/No)
Distribution	VDss (human)	-0.528	Numeric (log L/kg)
Distribution	Fraction unbound (human)	0.051	Numeric (Fu)
Distribution	BBB permeability	-0.195	Numeric (log BB)
Distribution	CNS permeability	-1.707	Numeric (log PS)
Metabolism	CYP2D6 substrate	No	Categorical (Yes/No)
Metabolism	CYP3A4 substrate	Yes	Categorical (Yes/No)
Metabolism	CYP1A2 inhibitor	Yes	Categorical (Yes/No)
Metabolism	CYP2C19 inhibitor	No	Categorical (Yes/No)
Metabolism	CYP2C9 inhibitor	No	Categorical (Yes/No)
Metabolism	CYP2D6 inhibitor	No	Categorical (Yes/No)
Metabolism	CYP3A4 inhibitor	No	Categorical (Yes/No)
Excretion	Total Clearance	1.832	Numeric (log ml/min/kg)
Excretion	Renal OCT2 substrate	No	Categorical (Yes/No)
Toxicity	AMES toxicity	No	Categorical (Yes/No)
Toxicity	Max. tolerated dose (human)	-0.791	Numeric (log mg/kg/day)
Toxicity	hERG I inhibitor	No	Categorical (Yes/No)
Toxicity	hERG II inhibitor	No	Categorical (Yes/No)
Toxicity	Oral Rat Acute Toxicity (LD50)	1.406	Numeric (mol/kg)
Toxicity	Oral Rat Chronic Toxicity (LOAEL)	3.33	Numeric (log mg/kg_bw/day)
Toxicity	Hepatotoxicity	No	Categorical (Yes/No)
Toxicity	Skin Sensitisation	Yes	Categorical (Yes/No)
Toxicity	<i>T.Pyriformis</i> toxicity	0.65	Numeric (log ug/L)
Toxicity	Minnow toxicity	-1.565	Numeric (log mM)

Table 4: Summative Physicochemical, Druggable, ADMET Properties of SA

Property	Value	
Molecular weight	284.48 g/mol	
LogP	6.03	
LogD	6.76	
LogSw	-5.51	
Number of stereocenters	0	
Stereochemical complexity	0.000	
Fsp3	0.944	
Topological polar surface area	26.30 Å ²	
Number of hydrogen bond donors	0	
Number of hydrogen bond acceptors	2	
Number of smallest set of smallest rings (SSSR)	0	
Size of the biggest system ring	0	
Number of rotatable bonds	15	
Number of rigid bonds	1	
Number of charged groups	0	
Total charge of the compound	0	
Number of carbon atoms	18	
Number of heteroatoms	2	
Number of heavy atoms	20	
Ratio between the number of non-carbon atoms and the number of carbon atoms	0.11	
Druggability Properties		
Lipinski's rule of 5 violations	1	
Veber rule	Good	
Egan rule	Good	
Oral PhysChem score (Traffic Lights)	4	
GSK's 4/400 score	Good	
Pfizer's 3/75 score	Bad	
Weighted quantitative estimate of drug-likeness (QEDw) score	0.213	
Solubility	1148.54	
Solubility Forecast Index	Reduced	
ADMET Properties		
Property	Value	
Human Intestinal Absorption	HIA+	0.994
Blood Brain Barrier	BBB+	0.986
Caco-2 permeable	Caco2+	0.801
P-glycoprotein substrate	Non-substrate	0.708
P-glycoprotein inhibitor I	Non-inhibitor	0.913
P-glycoprotein inhibitor II	Non-inhibitor	0.889
CYP450 2C9 substrate	Non-substrate	0.870
CYP450 2D6 substrate	Non-substrate	0.892
CYP450 3A4 substrate	Non-substrate	0.643
CYP450 1A2 inhibitor	Inhibitor	0.500
CYP450 2C9 inhibitor	Non-inhibitor	0.928
CYP450 2D6 inhibitor	Non-inhibitor	0.923
CYP450 2C19 inhibitor	Non-inhibitor	0.939
CYP450 3A4 inhibitor	Non-inhibitor	0.951
CYP450 inhibitory promiscuity	Low CYP Inhibitory Promiscuity	0.852
Ames test	Non AMES toxic	0.963
Carcinogenicity	Non-carcinogens	0.575
Biodegradation	Ready biodegradable	0.937
Rat acute toxicity	1.328 LD50, mol/kg	NA
hERG inhibition (predictor I)	Weak inhibitor	0.929
hERG inhibition (predictor II)	Non-inhibitor	0.849

Table 5 Performance measures of vNN models in 10-fold cross validation using a restricted or unrestricted applicability domain

Model	Data ^a	d ₀ ^b	h ^c	Accuracy	Sensitivity	Specificity	kappa	R ^d	Coverage
DILI	1427	0.60	0.50	0.71	0.70	0.73	0.42		0.66
		1.00	0.20	0.67	0.62	0.72	0.34		1.00
Cytotox (hep2g)	6097	0.40	0.20	0.84	0.88	0.76	0.64		0.89
		1.00	0.20	0.84	0.73	0.89	0.62		1.00
HLM	3219	0.40	0.20	0.81	0.72	0.87	0.59		0.91
		1.00	0.20	0.81	0.70	0.87	0.57		1.00
CYP1A2	7558	0.50	0.20	0.90	0.70	0.95	0.66		0.75
		1.00	0.20	0.89	0.61	0.95	0.60		1.00
CYP2C9	8072	0.50	0.20	0.91	0.55	0.96	0.54		0.76
		1.00	0.20	0.90	0.44	0.96	0.46		1.00
CYP2C19	8155	0.55	0.20	0.87	0.64	0.93	0.58		0.76
		1.00	0.20	0.86	0.52	0.94	0.50		1.00
CYP2D6	7805	0.50	0.20	0.89	0.61	0.94	0.57		0.75
		1.00	0.20	0.88	0.52	0.95	0.51		1.00
CYP3A4	10373	0.50	0.20	0.88	0.76	0.92	0.68		0.78
		1.00	0.20	0.88	0.69	0.93	0.64		1.00
BBB	353	0.60	0.20	0.90	0.94	0.86	0.80		0.61
		1.00	0.10	0.82	0.88	0.75	0.64		1.00
Pgp Substrate	822	0.60	0.20	0.79	0.80	0.79	0.58		0.66
		1.00	0.20	0.73	0.73	0.74	0.47		1.00
Pgp Inhibitor	2304	0.50	0.20	0.85	0.91	0.73	0.66		0.76
		1.00	0.10	0.81	0.86	0.74	0.61		1.00
hERG	685	0.70	0.70	0.84	0.84	0.83	0.68		0.80
		1.00	0.20	0.82	0.82	0.83	0.64		1.00
MMP	6261	0.50	0.40	0.89	0.64	0.94	0.61		0.69
		1.00	0.20	0.87	0.52	0.94	0.50		1.00
AMES	6512	0.50	0.40	0.82	0.86	0.75	0.62		0.79
		1.00	0.20	0.79	0.82	0.75	0.57		1.00
MRTD ^e	1184	0.60	0.20					-0.79	0.69
		1.00	0.20					-0.74	1.00